

Adaptation of *Arabidopsis halleri* to extreme metal pollution through limited metal accumulation involves changes in cell wall composition and metal homeostasis

Massimiliano Corso^{1,2} , Xinhui An¹ , Catherine Yvonne Jones³ , Verónica Gonzalez-Doblas² ,
M. Sol Schwartzman⁴ , Eugeniusz Malkowski⁵ , William G. T. Willats³ , Marc Hanikenne⁴  and
Nathalie Verbruggen¹ 

¹Laboratory of Plant Physiology and Molecular Genetics, Université Libre de Bruxelles, Brussels 1050, Belgium; ²Institut Jean-Pierre Bourgin, Université Paris-Saclay, INRAE, AgroParisTech, Versailles 78000, France; ³School of Natural and Environmental Sciences, Newcastle University, Newcastle upon Tyne, NE1 7RU, UK; ⁴InBioS-PhytoSystems, Functional Genomics and Plant Molecular Imaging, University of Liège, Liège B-4000, Belgium; ⁵Plant Ecophysiology Team, Institute of Biology, Biotechnology and Environmental Protection, Faculty of Natural Sciences, University of Silesia in Katowice, Katowice 40-032, Poland

Summary

Authors for correspondence:
Massimiliano Corso
Email: massimiliano.corso@inrae.fr

Nathalie Verbruggen
Email: nverbru@ulb.ac.be

Received: 15 May 2020
Accepted: 22 December 2020

New Phytologist (2021) 230: 669–682
doi: 10.1111/nph.17173

Key words: *Arabidopsis*, cadmium exclusion, cell wall, ion transport, ionomic, metal homeostasis, transcriptomic.

- Metallophytes constitute powerful models for the study of metal homeostasis, adaptation to extreme environments and the evolution of naturally selected traits. *Arabidopsis halleri* is a pseudometallophyte which shows constitutive zinc/cadmium (Zn/Cd) tolerance and Zn hyperaccumulation but high intraspecific variability in Cd accumulation.
- To examine the molecular basis of the variation in metal tolerance and accumulation, ionome, transcriptome and cell wall glycan array profiles were compared in two genetically close *A. halleri* populations from metalliferous and nonmetalliferous sites in Northern Italy. The metallicolous population displayed increased tolerance to and reduced hyperaccumulation of Zn, and limited accumulation of Cd, as well as altered metal homeostasis, compared to the nonmetallicolous population. This correlated well with the differential expression of transporter genes involved in trace metal entry and in Cd/Zn vacuolar sequestration in roots. Many cell wall-related genes were also more highly expressed in roots of the metallicolous population.
- Glycan array and histological staining analyses demonstrated that there were major differences between the two populations in terms of the accumulation of specific root pectin and hemicellulose epitopes.
- Our results support the idea that both specific cell wall components and regulation of transporter genes play a role in limiting accumulation of metals in *A. halleri* at contaminated sites.

Introduction

Trace metals such as cadmium (Cd) and zinc (Zn) are found widely in nature, and their soil concentrations have been shown to be susceptible to major anthropogenic disturbances (Tóth *et al.*, 2016). Zinc is an essential element with multiple biological functions, while Cd has no nutritional relevance in plants, and its presence, even in trace amounts, can be toxic (Broadley *et al.*, 2007; Clemens *et al.*, 2013; Clemens & Ma, 2016). Human exposure to an excess of trace metals mainly arises from contaminated food and to a lesser extent polluted air and water (Tóth *et al.*, 2016). Cadmium can be carcinogenic and can damage organs (in particular the kidneys, liver, and the reproductive and nervous systems) and cause mineral element deficiencies (Su *et al.*, 2014; Jan *et al.*, 2015).

Among the plants that can live on soils heavily polluted by trace metals, a rare class, called hyperaccumulators, is able to

accumulate extraordinarily high concentrations of these metals in above-ground tissues without toxicity symptoms. The pseudometallophyte and metal hyperaccumulator species *Arabidopsis halleri* is one of the best models with which to study metal homeostasis and adaptation to extreme environments (Verbruggen *et al.*, 2009, 2013; Krämer, 2010; Hanikenne & Nouet, 2011). *Arabidopsis halleri* populations are found throughout Europe. Phylogeographic studies have suggested the existence of several genetic units (GUs), each including both metallicolous (established on contaminated soils, M) and nonmetallicolous (established on noncontaminated soils, NM) populations: south-east (SE), north-west (NW) and hybrid zone (HZ) (Pauwels *et al.*, 2012; Meyer *et al.*, 2015; Wasowicz *et al.*, 2016). Within GUs, M populations seem to have derived from NM populations (Pauwels *et al.*, 2012), although there are exceptions (Babst-Kostecka *et al.*, 2018). While Zn hyperaccumulation is a constitutive trait in the species, Cd accumulation is highly variable

among *A. halleri* populations (Meyer *et al.*, 2015; Stein *et al.*, 2016). Cadmium and Zn hypertolerance and hyperaccumulation in *A. halleri* are driven by the high expression of genes involved in root uptake (e.g. *ZIP* members), root-to-shoot translocation (e.g. *Heavy Metal ATPase 4*, *HMA4*; *Nicotianamine synthase 2*, *NAS2*), and vacuolar sequestration of trace metals (e.g. *HMA3*, *CATION EXCHANGER (CAX) 2* and *4*; *Metal Transporter Protein 1*, *MTP1*) (Becher *et al.*, 2004; Hanikenne *et al.*, 2008; Fasani *et al.*, 2017; Corso *et al.*, 2018; Schwartzman *et al.*, 2018; Lee *et al.*, 2019). However, it remains unclear whether these genes contribute to the local adaptation of M populations to the contaminated environment or whether they are involved in constitutive tolerance capacities shared by M and NM populations (Meyer *et al.*, 2016). There is evidence that high expression of *HMA4* is constitutive in the *A. halleri* species, while that of *MTP1* may be the result of the evolution of secondary tolerance mechanisms (Meyer *et al.*, 2016). In addition, a major role of the cell wall in Cd accumulation and tolerance has also been suggested in *A. halleri* (Meyer *et al.*, 2015; Corso *et al.*, 2018), although there is lack of information about the composition of the cell wall and the expression of cell wall-related genes in *A. halleri* populations showing contrasting Cd and Zn accumulation and tolerance.

Recently, we examined the mechanisms underlying Cd and Zn tolerance and accumulation in two M populations of *A. halleri* from distinct GUs (SE and HZ) and highlighted contrasting Cd/Zn accumulation capacities, differences in the ability to adjust micronutrient homeostasis upon high Zn or Cd exposure, and a new role of flavonols in the adaptation to Cd exposure among populations (Corso *et al.*, 2018; Schwartzman *et al.*, 2018).

This article compares the ionomes, transcriptomes and cell wall compositions of two populations from different edaphic types (i.e. M and NM populations) within the same GU (SE, Northern Italy). Compared to the NM population, the M population has evolved reduced Zn and Cd accumulation and enhanced Zn and Cd tolerance through limited uptake and translocation, enhanced root vacuolar sequestration and modified cell wall composition and structure.

Materials and Methods

Seed, soil and plant material

Arabidopsis halleri I16 M and I30 NM plants and seeds, as well as soil samples, were harvested in Northern Italy (SE GU; Pauwels *et al.*, 2012; Supporting Information Fig. S1a) in July 2015. Shoots of 8–10 plants were subjected to mineral analysis. Soil (100–200 g dry weight per sample) was collected and pH and electrical conductivity were analysed as described in Corso *et al.*, (2018).

Physicochemical analysis and metal quantification in field samples

Sample digestion and mineral element quantification of I16 M and I30 NM shoots and soils collected *in situ* were performed according to Corso *et al.* (2018).

Experimental design of hydroponic culture

I16 M and I30 NM seeds were sown on vermiculite in a controlled growth chamber (Corso *et al.*, 2018). After 4 wk of growth, plants were transferred into a glasshouse (100 $\mu\text{mol photons m}^{-2}\text{s}^{-1}$ irradiance) in 4 l vessels filled with a hydroponic nutrient solution. Plants were then divided into two groups and transferred in the hydroponic solutions (Table S1) as described in Corso *et al.* (2018; design 1) and Schwartzman *et al.* (2018; design 2). After 4 wk (design 1) or 5 wk (design 2), 90 plants for each group and population were used for the growth test. Half of the plants (45 individuals) were transferred to vessels containing 5 $\mu\text{M CdSO}_4$ (design 1) and 150 $\mu\text{M ZnSO}_4$ (design 2), while the others were kept in their respective control solutions (Fig. 1a). From this point we will refer to the two groups as design 1-Cd and design 2-Zn.

Plants from design 1-Cd and design 2-Zn originated from the same batch of seeds, which were sown and grown together in the same glasshouse, following the same protocols.

Roots and shoots of three biological replicates (pools of 15 and 10 plants per replicate for design 1-Cd and 2-Zn, respectively) were harvested either 10 d (design 1-Cd) or 15 d (design 2-Zn) after stress initiation. Tissues were ground in liquid nitrogen and kept at -80°C for ionic, transcriptomic and glycan array analyses. Relative Chl content, shoot area and mineral elements were determined as described in Corso *et al.* (2018).

RNA extraction and mRNA-Seq analysis

Total RNA was extracted from 100 mg of ground frozen root and shoot samples using a Maxwell LEV Plant RNA Kit (Promega). RNA was quantified using a NanoDrop 2000 UV-Vis Spectrophotometer (Thermo Scientific, Loughborough, UK). Library preparation and RNA-Seq analyses were performed as described in Corso *et al.* (2018) and Schwartzman *et al.* (2018). The *A. halleri* reference transcriptome used in this study is described in Schwartzman *et al.* (2018). The RNA sequencing data have been deposited at the National Center for Biotechnology Information Transcriptome Shotgun Assembly Sequence Database (TSA) with BioProject identification nos. PRJNA388549 and PRJNA564209.

Statistical analysis and data mining on RNA-Seq data

Statistical analyses were performed to identify Differentially Expressed Genes (DEGs) using the DESeq2 R package (Love *et al.*, 2014). Pairwise comparisons were carried out to identify DEGs with the following thresholds: \log_2 fold change (FC) > 0.5 and < -0.5 and false discovery rate (FDR) < 0.05 . A first comparison was aimed at evaluating the effect of the edaphic type (ET), and key mechanisms of adaptation to metalliferous soils were identified which did not depend on the precise age or differences in concentrations of some nutrients in the medium. In particular, an I16 M versus I30 NM comparison considering together control and treated conditions of both design 1-Cd and 2-Zn for each genotype (six samples for

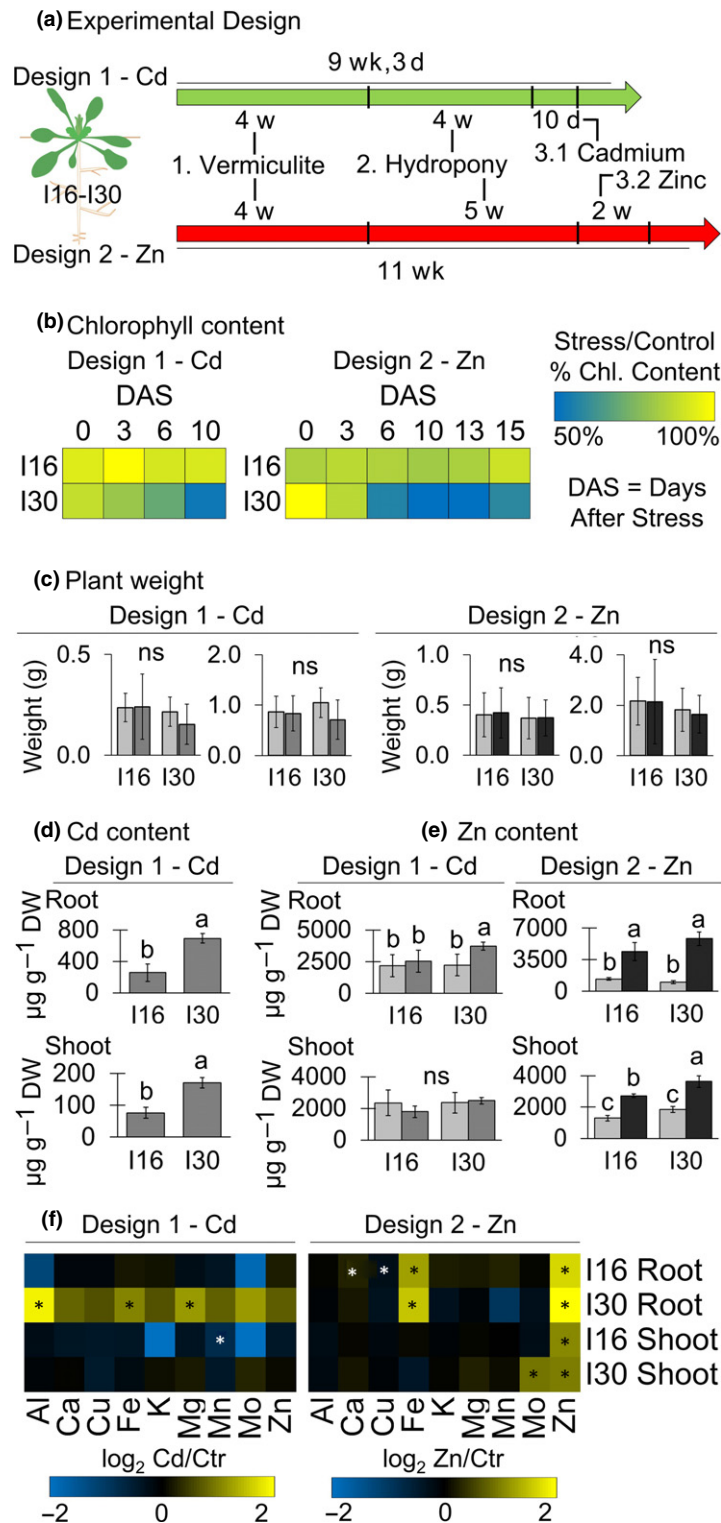


Fig. 1 Physiological and ionic analysis of *Arabidopsis halleri* plants. (a) Experimental design of hydroponic cultures with *A. halleri* populations. (b) Chlorophyll content, represented as $\log_2(\text{stress/control plants})$, and (c) root and shoot weights were measured in control, and Cd- and Zn-treated plants. Error bars represent the SD ($n = 25\text{--}30$). DAS, days after stress; ns, not significant. (d) Cadmium concentration in I16 M and I30 NM Cd-treated roots and shoots (three biological replicates) measured after 10 d in hydroponic solution containing $5 \mu\text{M CdSO}_4$. (e) Zinc concentration in I16 M and I30 NM control and Zn-treated roots and shoots (three biological replicates) measured after 14 d in hydroponic solution containing $150 \mu\text{M ZnSO}_4$. Different letters indicate statistically significant differences ($P \leq 0.05$) according to ANOVA with Tukey's range test. Error bars represent the SD. (f) Heatmaps representing $\log_2(\text{Cd-stress/control})$ and $\log_2(\text{Zn-stress/control})$ of essential mineral element concentrations in I16 M and I30 NM plants (three biological replicates). Asterisks indicate statistically significant differences ($*$, $P < 0.05$), assessed by ANOVA with Tukey's range test.

design 1-Cd and six samples for design 2-Zn for each genotype). The statistical analyses used to identify the core DEGs between the two populations were very robust, since the numbers of samples taken into account for the comparison (12 samples for I16 M and 12 samples for I30 NM) were significantly higher than the usual three replicates considered in most transcriptomic studies (McCarthy *et al.*, 2012; Love *et al.*, 2014). A second comparison was aimed at evaluating the effect of the treatment (T) – that is, a control versus treatment comparison within both design 1-Cd and design 2-Zn for each genotype. In both analyses, root and shoot RNA-Seq expression data were considered separately. These comparisons allowed evaluation of the weight of each factor (ET vs T) on differential gene expression. Gene Ontology (GO) enrichment analyses were performed for each DEG set using the CLUEGO ‘cytoscape’ plugin (Bindea *et al.*, 2009) with the built-in Fisher’s exact test function and an adjusted *P*-value < 0.01.

Heatmap and hierarchical clustering analyses were carried out using the ‘heatmap.2’ function (GPLTS R package). The principal component analysis (PCA) was carried out using the ‘prcomp’ R function.

cDNA synthesis and real-time quantitative polymerase chain reaction (qRT-PCR) analysis

Real-time quantitative PCR analysis was carried out according to the method described by Corso *et al.* (2018). Primers for qRT-PCR are listed in Table S2.

Cell wall pectins and hemicellulose quantification

The crude cell walls of I16 M and I30 NM *A. halleri* roots were prepared and fractionated into pectin, hemicellulose 1 (HC1) and hemicellulose 2 (HC2) fractions as described by Zhong & Lauchli (1993) and Fang *et al.*, (2012), with modifications. Briefly, 150 mg of root material was homogenized with 2 ml ice-cold 75% ethanol for 20 min, then washed three times with 2 ml ice-cold acetone, 2 ml ice-cold methanol : chloroform (1 : 1) and 2 ml ice-cold methanol for 20 min each. The supernatant was discarded after 10 min centrifugation at 8000 g at 4°C. The pellets containing the extracted cell walls were freeze dried overnight and stored at 4°C.

The pectin fraction was obtained by incubating two aliquots of 2 mg of the extracted cell walls with 1 ml 0.5% ammonium oxalate buffer (0.1% NaBH₄) at 100°C for 1h. The supernatants from the two aliquots were cooled, combined and adjusted to 2 ml volume with ammonium oxalate buffer after 10 min of centrifugation at 13 800 g. The pellets were washed with double-distilled water (ddH₂O) and subsequently extracted with 1 ml 4% NaOH (0.1% NaBH₄) for 24 h at room temperature; the supernatant contained the hemicellulose 1 fraction. The hemicellulose 2 fraction was extracted in a similar way, using 1 ml 24% NaOH (0.1% NaBH₄).

The cell wall uronic acid content was assayed as described by Blumenkrantz & Asboe-Hansen (1973), using galacturonic acid as a standard. Different aliquots (0, 20, 40, 60, 80, 100, 200 µl)

of 0.1 µg µL⁻¹ galacturonic acid solution were transferred to 1.5 ml tubes and the volume was adjusted to 200 µl with ddH₂O to make the standard curve. Briefly, 100 µl extracts were incubated at 100°C for 5 min with 500 µl 98% H₂SO₄ (containing 0.0125M Na₂B₄O₇) in glass tubes. After cooling, 10 µL m-hydroxydiphenyl (0.15%) was added to the solution. The extracts were incubated for 20 min at room temperature, and the absorbance was then measured at 520 nm using a BioTek Gen5 Plate Reader (BioTek Instruments, Colmar Cedex, France).

Total polysaccharide content was determined via the phenol sulfuric acid method (Dubois *et al.*, 1951; Shi *et al.*, 2015). Different aliquots (0, 20, 40, 60, 80, 100, 200 µl) of 1 µg µL⁻¹ glucose solution were transferred to 1.5 ml tubes and the volume was adjusted to 200 µl with ddH₂O to make the standard curve. Briefly, 200 µl extracts were incubated with 500 µl 98% H₂SO₄ and 5 µl 80% phenol in glass tubes at room temperature for 15 min, then incubated at 100°C for 15 min. After cooling, 200 µl solution was added to 96 well plates and the absorbance at 490nm was measured using the BioTek Gen5 Plate Reader.

Cell wall glycan array and histological staining

Alcohol insoluble residue (AIR) was prepared from 10 mg of (freeze dried) root tissue and used for sequential extraction of pectins and hemicelluloses according to the method described by Moller *et al.* (2007). Briefly, pectins and hemicelluloses were sequentially extracted from 10mg AIR using 30 µl mg⁻¹ of 50mM cyclohexane-diamine-tetraacetic acid (CDTA), then with 30 µl mg⁻¹ 4M NaOH in 0.1% NaBH₄ (w/v) respectively. Extracts were printed onto nitrocellulose membrane using a Sprint micro-array robot (Arrayjet, Roslin, UK) in four concentrations following a 10× dilution series (diluted with glycerol buffer: 47% glycerol, 0.06% Triton, 0.04% Proclin 200) and two technical replicates. Arrays were blocked with 5% milk protein TBS buffer with 0.1% Tween-20 (v/v, MP-TBST), probed with rat conjugated primary antibodies (from Plant Probes, diluted 1 : 10 in MP-TBST buffer) for 1.5 h. They were then washed three times in TBST (15 min per wash), probed with anti-rat alkaline phosphatase secondary antibodies (Sigma, diluted 1 : 200 MP-TBST), washed three times in dH₂O (15 min per wash), and stained using nitroterazolium blue chloride/5-bromo-4-chloro-3-indolyl phosphate (NBT/BCIP) standard protocol (Sigma). Probed arrays were scanned at 2400 dpi using a Canon 9000F Mark II flatbed scanner (Canon, Uxbridge, UK) and images were analyzed with ARRAY-PRO ANALYZER (v.6.3.1) to generate spot signal values that were used to produce a heatmap integrated with hierarchical clustering.

Cell wall and lignin histological staining were carried out on I16 M and I30 NM roots according to the methods described by Ursache *et al.* (2018). Plants were grown in ½ Murashige & Skoog medium or ½MS + 50 µM CdSO₄ (no sugar added, as in Barberon *et al.*, 2016) for 7 d. Plants were stained with calcofluor white and basic fuchsin to visualize cell walls and lignin, respectively. Roots were analysed using a

Leica SP8 AOBS Tandem HyD confocal microscope ($\times 63$ magnification; Leica, Paris, FR) following the protocol described by Ursache *et al.* (2018). In order to compare the different plants, the images were always taken at the same root section, at 10–15 cells after the onset of the Casparian strip formation. Eight biological replicates were used for I16 M and I30 NM samples, while three biological replicates were used for Col-0.

Cadmium staining (Leadmium Green)

For *in vitro* growth, seeds of I16 M and I30 NM plants were sterilized and grown in $\frac{1}{2}$ MS or $\frac{1}{2}$ MS + 50 μ M CdSO₄ for 7 d, using the same conditions described for the histological staining. Leadmium Green Cd fluorescent dye (Fisher Scientific, Merelbeke, Belgium) was used to investigate the distribution of Cd in I16 M and I30 NM roots of plants grown *in vitro*. The entire roots were stained with Leadmium Green (diluted 1:10 in 0.85% NaCl solution) for 90 min in the dark, then washed with a 0.85% NaCl solution for 10 min. Cadmium was visualized using a Leica SP5 inverted confocal microscope with excitation and emission wavelengths of 488 and 515 nm, respectively.

Statistical analysis on physiological, ionic and glycan array data

To assess statistical differences in physiological parameters (Chl content, growth, weight) and mineral element concentration among *A. halleri* populations, a *t*-test (Cd vs control or shoot vs root) and ANOVA (differences among populations) with Tukey's range test ($P < 0.05$) were performed using the AGRICOLA R package.

Results

Soil and shoot mineral profiles of geographically close M and NM *Arabidopsis halleri* populations from field samples

Two *A. halleri* populations from the south-east genetic unit (Northern Italy), I16 M and I30 NM, were used in this study (Pauwels *et al.*, 2012; Frérot *et al.*, 2017). I16 M grows near a factory which uses powder residues derived from steel production, while I30 NM grows in a noncontaminated area 60 km away from I16 M (Fig. S1a). I16 M behaved as a Zn hyperaccumulator and limited Cd accumulator, showing concentrations in shoots higher than the 3000 ppm Zn and lower than the 100 ppm Cd hyperaccumulation thresholds (Fig. S1b,c; Corso *et al.*, 2018). By contrast, I30 NM, which grows in a soil with almost no Cd, and much lower Zn and copper (Cu) concentrations, accumulated as much Zn, and higher Cu concentrations, in shoots than I16 M (Fig. S1b). The Zn bioaccumulation factor (BF), that is, the ratio between the shoot metal content and the bioavailable metal in the soil, was 1026 in I30 NM and 6 in I16 M (Fig. S1d), while the Cd BF was 24 for the I16 M population.

Contrasting ionic profiles between I16 M and I30 NM plants grown in hydroponic culture

The I16 M and I30 NM populations were further compared for metal tolerance and accumulation (Fig. 1a). Plant growth was measured in two control hydroponic solutions and conditions used in our previous studies (Corso *et al.*, 2018 and Schwartzman *et al.*, 2018; Table S1). Hence, treatments with 5 μ M Cd for 10 d in solution 1, named (design 1-Cd) (Corso *et al.*, 2018), or with 150 μ M Zn for 14 d in solution 2, named (design 2-Zn) (Schwartzman *et al.*, 2018), were applied (Fig. 1a).

Cadmium- and Zn-treated I30 NM plants showed a significant reduction in Chl content with respect to the control plants, which is a typical symptom of metal toxicity, while in I16 M Chl concentrations in metal-treated and control plants were similar (Fig. 1b). At the end of the treatments, root and shoot biomass did not significantly differ between control and treated samples in both populations (Fig. 1c). I30 NM accumulated more Cd than I16 (design 1-Cd) in both roots and shoots (Fig. 1d). Remarkably, I30 NM accumulated significantly higher Zn concentrations than I16 in shoots when plants were exposed to high Zn (design 2-Zn) and in roots when plants were exposed to high Cd (design 1-Cd) (Fig. 1e). No difference in Zn concentration in tissues was observed in control conditions.

In addition, the Cd treatment impacted the concentrations of other mineral elements and enhanced the accumulation of most metals in I30 NM roots, while I16 M was characterized by a global decrease of all mineral elements in roots (Fig. 1f). Instead, I16 M and I30 NM roots subjected to high Zn both showed higher iron (Fe) accumulation compared to the control condition, and this was more pronounced for I30 NM (Fig. 1f).

Transcriptomic profiles in I16 M and I30 NM plants

The molecular basis underlying the contrasting behaviours of I16 M and I30 NM was investigated by RNA-Seq of roots and shoots from plants grown in control and metal-contaminated (Zn or Cd) conditions (48 samples; Fig. 1a; Table S3a,b). A PCA conducted on RNA-Seq data showed that the growth conditions associated with designs 1-Cd and 2-Zn constituted the factor (PC1) with the strongest impact on gene expression profiles of roots and shoots (Fig. 2a). The edaphic type (i.e. M vs NM) was the second factor (PC2) affecting expression, while the metallic treatments had a very limited effect.

The genes which were more highly expressed in plants grown under design 1-Cd than design 2-Zn included those with roles in photosynthesis, cell cycle and transport. Conversely, the genes which were more highly expressed in plants grown under design 2-Zn than design 1-Cd belonged to abiotic and biotic stress response categories (Fig. 2b).

Although major differences in the transcriptome profiles were observed between the two experimental designs, constitutive transcriptomic differences were identified between the two populations when all samples of roots and shoot (from the two designs, including controls and treatments; 12 samples for each population) were pooled for a pairwise comparison of gene expression

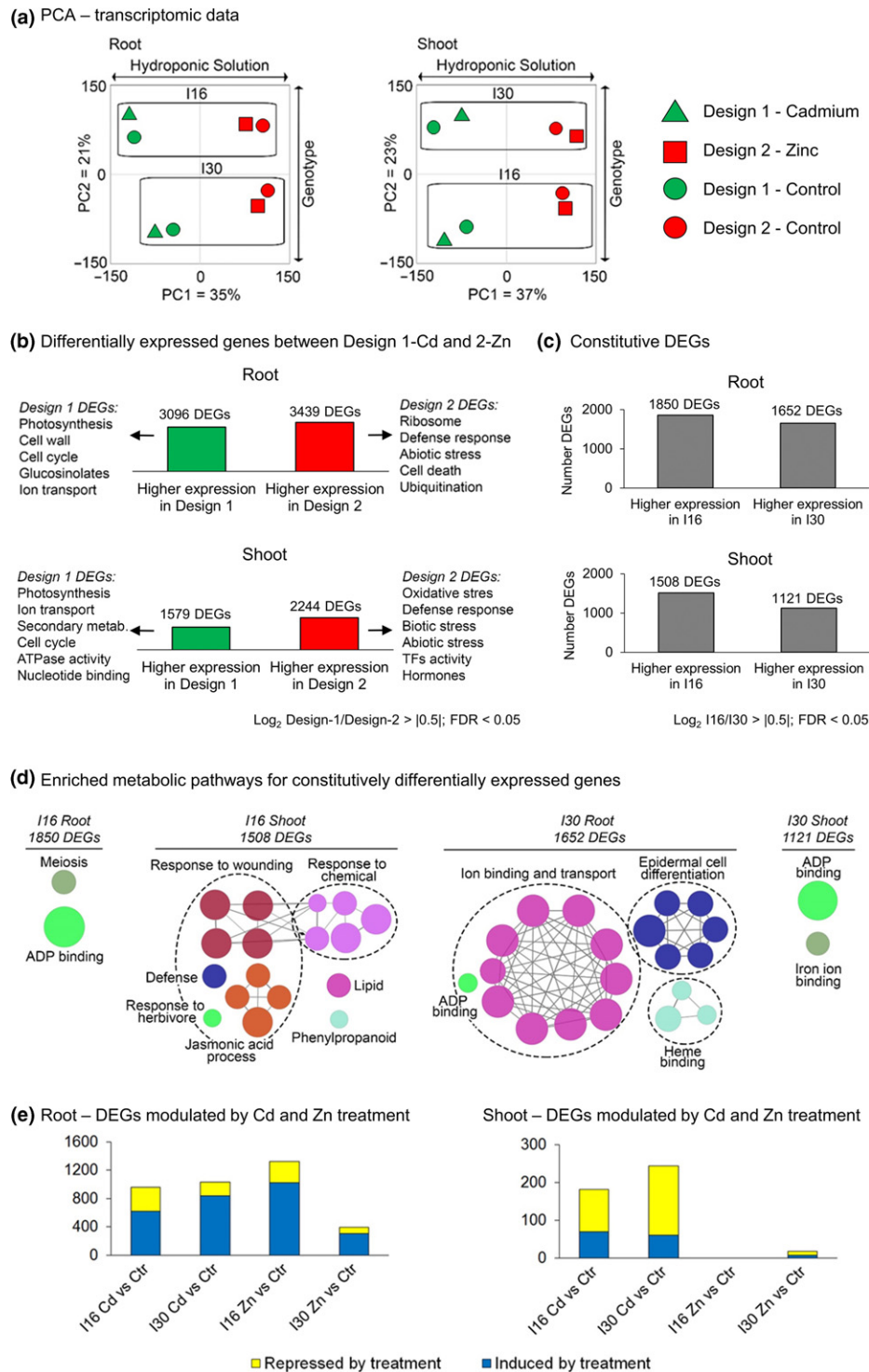


Fig. 2 Comparison of transcriptomic profiles in I16 M and I30 NM *Arabidopsis halleri* populations. (a) Principal component analysis (PCA) of transcriptomic data. I16 M and I30 NM sample distribution in roots and shoots according to PC1 and PC2. The percentage of variance is reported for each component. (b) Pairwise comparison with enriched metabolic pathways between design 1 and design 2 RNA-Seq data. The thresholds for selecting differentially expressed genes (DEGs) in design 1 vs design 2 (i.e. six control (I16 M and I30 NM) plus six metal-treated samples (I16 M and I30 NM for Zn and Cd) for each design) were $\log_2(\text{design 1/design 2})$ counts > 0.5 (genes with higher expression in design 1 than design 2) and < -0.5 (genes with higher expression in design 2 than design 1). The enriched metabolic pathways are shown. FDR, false discovery rate; TF, transcription factor. (c) Constitutively DEGs between I16 M and I30 NM. Pairwise comparison between I16 M and I30 NM RNA-Seq data. The thresholds for selecting DEGs in I16 M and I30 NM (i.e. six control plus six metal-treated samples for each population) were $\log_2(\text{I16 M/I30 NM})$ counts > 0.5 (genes with higher expression in I16 M than I30 NM) and < -0.5 (genes with higher expression in I30 NM than I16 M). FDR, false discovery rate. (d) Enriched metabolic pathways for constitutively expressed genes with higher expression in I16 M and I30 NM. (e) DEGs induced ($\log_2(\text{metal-stress/control}) > 0.5$) or repressed ($\log_2(\text{metal-stress/control}) < -0.5$) by Cd and Zn treatment.

($\log_2 I16/I30 > 0.5$ or < -0.5 ; Fig. 2c; Table S3c). According to GO term enrichment analyses, genes that were constitutively more highly expressed in I16 M than in I30 NM shoots were related to wounding, and to herbivore attack and jasmonic acid responses, whereas several genes which were more highly expressed in I30 NM than in I16 M were linked to ion binding/transport and epidermal cell differentiation in roots, and ADP/iron binding in shoots (Fig. 2d).

Additional pairwise comparisons confirmed that only a few genes were modulated by Cd or Zn treatments, and the number of genes modulated by both treatments in I16 M or I30 NM only represented a small percentage of the genes regulated by Cd or Zn alone (Fig. 2e).

The expression patterns of 10 representative genes were validated in I16 M and I30 NM shoot and root samples by qRT-PCR (Fig. S2a) and a high correlation between the RNA-Seq and qRT-PCR data was observed ($r=0.84$; $FDR < 2.1 \times 10^{-6}$; Fig. S2b), as already shown in Corso *et al.* (2018) and Schwartzman *et al.* (2018).

Among the core set of constitutive DEGs between I16 M and I30 NM in roots and/or in shoots, many encoded transporters or proteins involved in metal binding (Fig. 3). For instance, genes involved in root metal uptake (*IRON-REGULATED TRANSPORTER 1*, *IRT1*), nicotianamine (NA) synthesis (*NICOTIANAMINE SYNTHASE 4*, *NAS4*), NA and glutathione (GSH) transport (*YELLOW STRIPE like 7*, *YSL7* and *OLIGOPEPTIDE TRANSPORTER 3*, *OPT3*) showed lower expression in I16 M than in the I30 NM Cd/Zn hyperaccumulator. Conversely, I16 M exhibited higher and constitutive expression of genes involved in Cd/Zn vacuolar sequestration (*HEAVY METAL ATPase 3*, *HMA3* and *CATION/PROTON EXCHANGER 4*, *CAX4*) and metal chelation and detoxification (*ZINC INDUCED FACILITATOR 1*, *ZIF1*; *METALLOTHIONEIN 3*, *MT3*; *HEAVY METAL-ASSOCIATED ISOPRENYLATED PLANT PROTEINS*, *HIPP21*, *25* and *35*). Other genes showing higher expression in I16 M than in I30 NM shoots are those involved in metal remobilization (*HMA2* and *NATURAL RESISTANCE ASSOCIATED-MACROPHAGE PROTEIN3*, *NRAMP3*) (Fig. 3).

Besides transporter genes, several constitutive DEGs between I16 M and I30 NM roots were related to the cell wall (Fig. 4a). Hence, the expression of genes involved in the synthesis and regulation of arabinogalactan, extensin, galacturonan, pectin-methyl-esterase, xyloglucan and lignin cell wall components diverged in I16 M and I30 NM roots (Fig. 4a). Galacturonan genes, such as *GALACTAN SYNTHASE1* (*GALS1*), *ARABINAN DEFICIENT2* (*ARAD2*), *GALACTURONOSYLTRANSFERASE2* (*GAUT2*) and *GAUT-like6* (*GATL6*) showed higher expression in I16 M than in I30 NM roots (Fig. 4a). These genes are involved in rhamnogalacturonan biosynthesis (*GALS1*, *ARAD2*; Verherbruggen *et al.*, 2013) and in homogalacturonan biosynthesis (*GAUT2*, *GATL6*; Atmodjo *et al.*, 2013). Several lignin-related genes were also more highly expressed in I16 M than I30 NM roots, such as *ENHANCED SUBERIN 1* (*ESB1*), which in *Arabidopsis thaliana* drives the formation of the Casparian strip and is essential for the control of solute and metal movements in the endodermis (Hosmani *et al.*, 2013). Finally, some

PECTIN METHYLESTERASE (*PME*) genes were induced by Cd in I30 NM but not in I16 M (Fig. 4b).

Cell wall analyses in I16 M and I30 NM

The biochemistry of the cell wall was next examined using glycan profiling of plant cell wall polymers with high-resolution microarrays (Moller *et al.*, 2007, 2008), a technique allowing the characterization of cell wall composition using twenty monoclonal antibodies covering specifically the most abundant epitopes of cell wall components. It was used here to profile pectin and hemicellulose extracts in I16 M and I30 NM roots grown in control and Cd conditions (Fig. 4c). Most measured cell wall components had higher relative abundances in I16 M roots compared to I30 NM (Fig. 4d). Specifically, pectin arabinogalactan, extensin, (1 → 4)-β-galactan, (1 → 5)-α-arabinan and homogalacturonan showed a higher signal intensity in I16 M than in I30 NM roots. Pectin rhamnogalacturonans, as (1 → 4)-β-galactan (LM5) and (1 → 5)-α-arabinan (LM6), was found to be two to three times more abundant in I16 M than I30 NM (Fig. 4d). In the comparison between I16 M and I30 NM roots, pectins were the cell wall components that were most different, making them the most promising cell wall component candidates for involvement in the reduced metal accumulation strategy of I16 M. Higher relative signal intensities were also found for xyloglucan and mannan cell wall components in hemicellulose extracts of I16 M than in I30 NM control roots (Fig. 4c,d). The signal detected in pectin and hemicellulose extracts (Fig. 4c) decreased in Cd-treated samples of both I16 M and I30 NM compared to controls. This is most likely due to the fact that Cd leads to modifications of cell wall physicochemical properties (Parrotta *et al.*, 2015), resulting in poor recognition of the specific epitopes of cell wall components by antibodies on the glycan array.

To confirm this hypothesis, we measured the total pectin and hemicellulose contents in I16 M and I30 NM plants grown in control solution or under Cd stress, using the same samples analysed by RNA-Seq and glycan array analyses (Fig. S3). Our results showed that the total pectin content did not change significantly among genotypes and treatments. Hemicellulose 1 content was significantly higher in I16 plants treated with Cd compared to the other samples, while hemicellulose 2 was already higher in I16 than I30 in the control condition. Taken together, our results confirmed that neither total pectin content nor total hemicellulose content decreased under Cd treatment and that the differences observed in the glycan array are most likely related to recognition of the epitopes.

In addition, histological staining (Ursache *et al.*, 2018) was used to examine cell wall structure and lignin deposition in roots of I16 M and I30 NM grown *in vitro* on normal and Cd-supplemented media for 7 d (Fig. 4e,f). While Casparian strip organisation and lignin deposition were similar between the two populations and growing conditions (Fig. 4e), some differences were observed in root anatomy between I16 and I30. In particular, in most cases two cortex layers were observed in I16 roots and one cortical layer was present in I30 (Fig. 4f). Nevertheless,

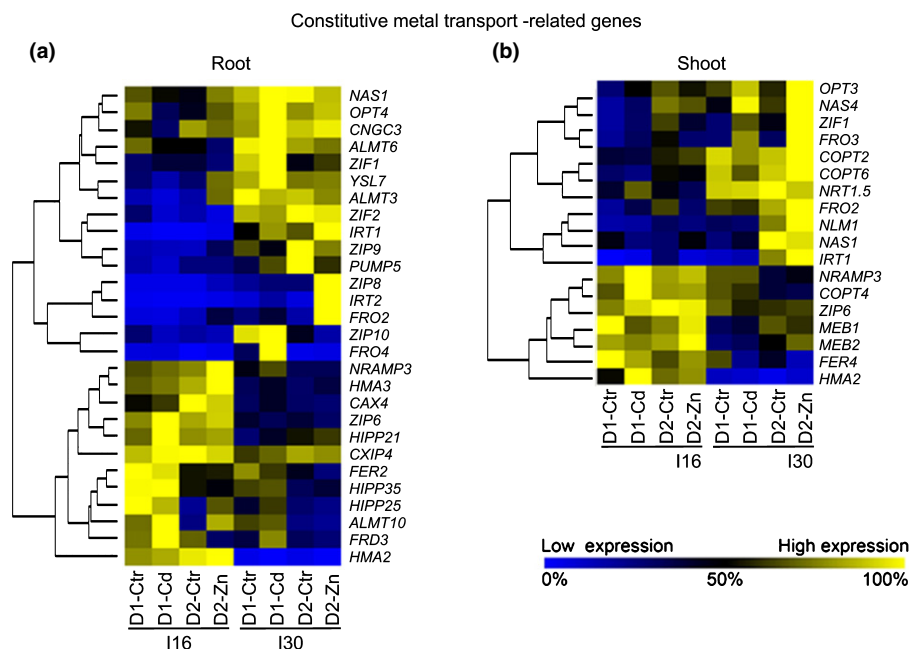


Fig. 3 Expression of metal transport-related genes in *Arabidopsis halleri* I16 M and I30 NM. (a, b) Heatmap of selected RNA-Seq data with transport-related genes that showed constitutive higher expression in I16 M ($\log_2(I16\ M/I30\ NM) > 0.5$) and I30 NM ($\log_2(I16\ M/I30\ NM) < -0.5$) (a) roots and (b) shoots of plants of designs 1 (D1) and 2 (D2). The expression values were calculated as percentages relative to the sample showing the highest expression value for each gene (100% and 0% are represented by yellow and blue colouring, respectively) within I16 M and I30 NM.

the number of root cortex layers varies according to the plants and/or the conditions, suggesting that *A. halleri* roots are characterised by high plasticity. Finally, Cd distribution was studied in roots of I16 M and I30 NM grown in the same conditions. Leadmium Green staining indicated higher accumulation of Cd in I30 NM than I16 M roots (Fig. S4). A weak fluorescent signal was also detected in roots in control conditions, which is most likely due to Leadmium Green binding to metals other than Cd, most likely Zn.

Discussion

With this study, we examined the physiological and molecular basis underlying contrasting metal accumulation and compared ionome, transcriptome and cell wall composition landscapes in two genetically close *A. halleri* populations: a nonmetallicolous

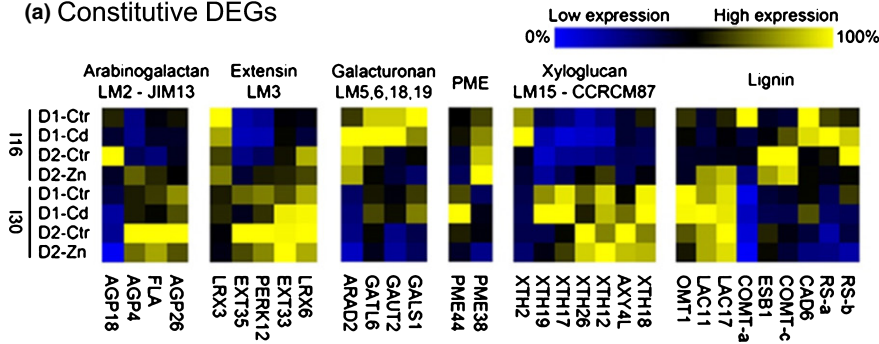
(I30 NM) population, and a metallicolous (I16 M) population, hypertolerant to Zn and Cd (Corso *et al.*, 2018; Schwartzman *et al.*, 2018).

Contrasting ionic profiles between I16 M and I30 NM plants

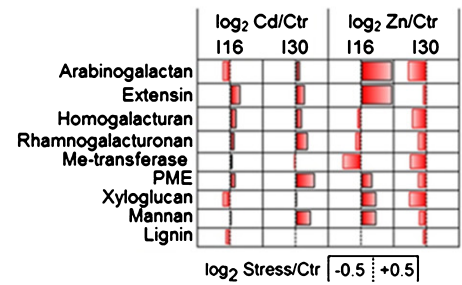
Ionic profiles of plants growing in the field or in hydropony suggested the activation of different strategies for metal accumulation and a general re-organisation of metal homeostasis in I16 M, which limits Cd and Zn entry in tissues, compared to I30 NM plants. These differences are particularly evident upon Cd stress in roots, where I16 M showed significantly lower accumulation of Fe, Mg and Al compared to I30 NM (Figs 1, S1). The I16 M and I30 NM ionome profiles are both very different from observations made in PL22, an *A. halleri* Cd/Zn hypertolerant

Fig. 4 Cell wall gene expression and composition in *Arabidopsis halleri* I16M and I30NM. (a) Heatmap of selected RNA-Seq data with cell wall related genes that showed constitutive higher expression in I16 M ($\log_2(I16\ M / I30\ NM) > 0.5$) and I30 NM ($\log_2(I16\ M / I30\ NM) < -0.5$) roots of plants under designs 1-Cd (D1) and 2-Zn (D2). The expression values were calculated as percentages relative to the sample showing the highest expression value for each gene (100% and 0% are represented by yellow and blue colouring, respectively) within I16 M and I30 NM. (b) Average expression of cell wall related gene categories in I16 M and I30 NM reported as $\log_2(\text{stress}/\text{control samples})$. (c, d) Cell wall composition of *A. halleri* roots. (c) Heatmap showing the accumulation of pectin and hemicellulose cell wall components identified using monoclonal antibodies (mAb; see the Materials and Methods section). The quantities are expressed as percentages relative to the sample showing the highest accumulation value for each antibody (100% and 0% are represented by yellow and blue colouring, respectively) within I16 M and I30 NM. (d) Cell wall components recognised by specific antibodies showing differential accumulation between I16 M and I30 NM. Different letters indicate statistically significant differences ($P \leq 0.05$) according to ANOVA with Tukey's range test. JIM, John Innes Monoclonal antibodies; LM, Leeds monoclonal antibodies. Error bars represent the SD. (e) Surface view maximum projection of Casparian strip lignin staining in the differentiated root zone of I16M and I30 NM plants grown in control and 50 μM Cd-contaminated $\frac{1}{2}$ Murashige & Skoog ($\frac{1}{2}$ MS) agar medium for 7 d. The spiral-like signal is from a deeper-lying xylem vessel. Bars, 45 μm . (f) Root transversal sections showing cell wall structures (blue) and lignin distribution (red) in I16M and I30NM plants grown in control and 50 μM Cd-contaminated $\frac{1}{2}$ MS agar medium for 7 d. Bars, 45 μm . The arrows indicate the root cortex layers.

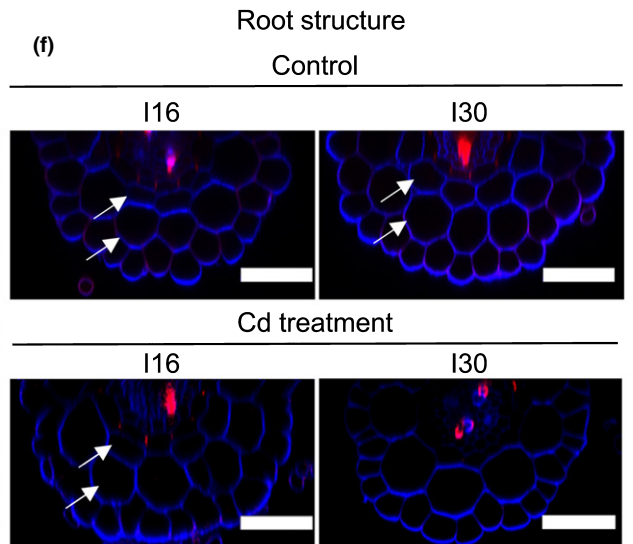
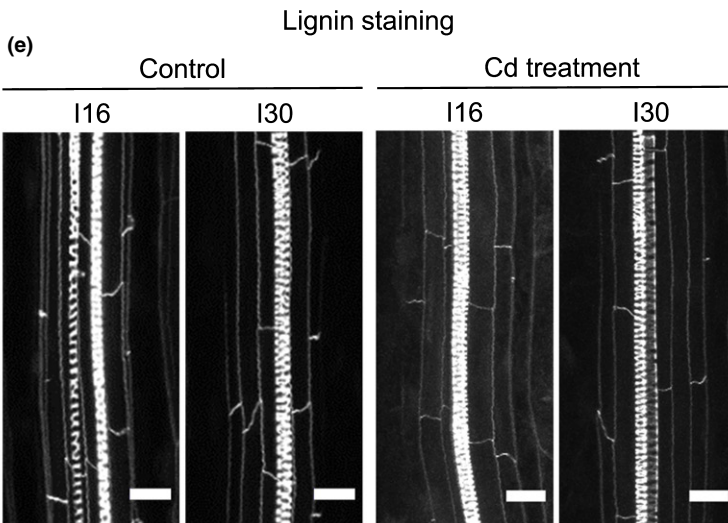
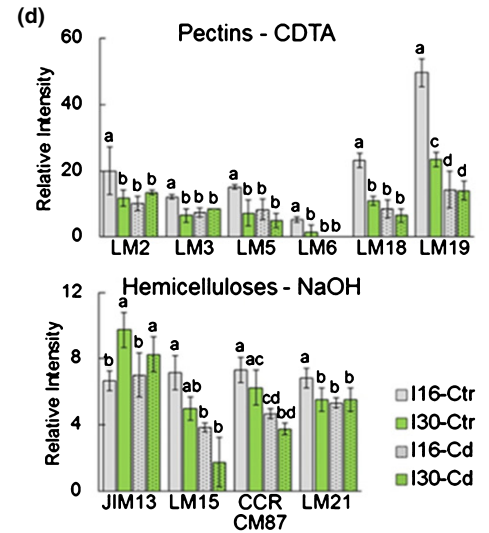
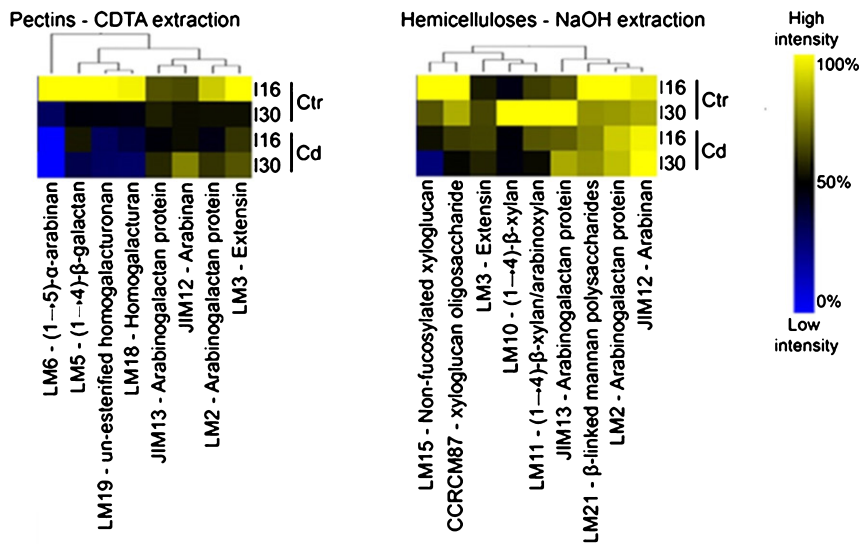
(a) Constitutive DEGs



(b) Average expression of CW genes



(c) Cell wall composition of *A. halleri* roots – glycan array



and hyperaccumulator metallicolous population from the HZ GU (Corso *et al.*, 2018). PL22 indeed showed higher concentrations of several micro- and macro-elements (Fe, Cu, Mg, K, S, P) in shoots of plants subjected to Cd exposure compared to the control plants. Thus, comparison of multiple *A. halleri*

populations highlighted contrasting accumulation strategies, and contrasting impacts of high Zn or Cd exposure on the ionome of the plants. This also suggested that distinct molecular mechanisms underlie those ionome differences, and these were examined using RNA-Seq analysis.

Major impact of the growing solutions on gene expression profiles and core differences between I16 M and I30 NM

The analysis of RNA-Seq data highlighted a major impact of the hydroponic solution on gene expression (Fig. 2a). Although it is well known that plants possess a high degree of plasticity that allows them to adapt their physiology in response to different environments and mineral element availability (Gruber *et al.*, 2013; Barberon *et al.*, 2016; Doblas *et al.*, 2017; Arnold *et al.*, 2019), changes in medium composition had here an effect largely exceeding those of the edaphic origin of the plants or exposure to toxic concentrations of Zn and Cd. These observations shed new light on the study of *Arabidopsis halleri* and suggest that careful comparison of data obtained in different studies is warranted.

The expression of several genes covering multiple biological pathways was changed by the composition of the growth solution (Fig. 2b). Those included pathways linked to specialized metabolites, ion transport and the cell wall in design 1-Cd, and to stress responses and transcription factor activity in design 2-Zn, suggesting a generalized impact of the growing solution on the transcriptomic profiles, which likely reflects the distinct steady-state physiology of each plant.

The iron content was different between design 1-Cd (20 μM of Fe-ethylenediamine-N,N'-bis(2-hydroxyphenyl)acetic acid, FeEDDHA) and design 2-Zn (10 μM of Fe-hydroxybenzyl ethylenediamine, FeHBED) solutions. Despite these differences, total Fe concentrations were similar in the plants (roots and shoots) grown in the two solutions.

In spite of the large impact of medium composition, an important set of genes with constitutive differences in expression between I16 M and I30 NM roots (3502 DEGs) and shoots (2629 DEGs) was identified and represented core differences among the two populations (Fig. 2c).

Metal transport strategies diverge between I16 M and I30 NM

We hypothesised that the higher Cd and Zn tolerance and reduced accumulation observed in the I16 M population compared to I30 NM is related to altered metal uptake and to detoxification mechanisms through Cd/Zn vacuolar sequestration in the root/lower translocation to the shoot and metal chelation (Fig. 3).

In the case of I16 M, the limited root Cd uptake might be linked to the lower expression of *AbIRT1* compared to I30 NM and PL22 (Corso *et al.*, 2018) *A. halleri* Cd hyperaccumulators. IRT1 mediates Fe and Cd uptake in *A. thaliana* roots (Vert *et al.*, 2002; Dubeaux *et al.*, 2018) and was hypothesized to control root Zn and Cd accumulation in *A. halleri* (Corso *et al.*, 2018; Schwartzman *et al.*, 2018) and *Noccaea caerulescens* (Halimaa *et al.*, 2019) Cd hyperaccumulators. IRT1 may also contribute to variation in nickel hyperaccumulation in *N. caerulescens* (Merlot *et al.*, 2018). Evidence is thus accumulating that IRT1 may be a major determinant of the intraspecific variation in metal accumulation observed in hyperaccumulators.

Besides the limited Cd uptake, metal vacuolar sequestration is enhanced and plays a major role in I16 M roots, as suggested by the higher expression of genes involved in Cd/Zn vacuolar

sequestration in I16 M than in I30 NM roots (*HMA3* and *CAX4*; Mei *et al.*, 2009; Liu *et al.*, 2017). In addition, I16 M might limit the accumulation of metals in the shoot tissue by lowering the expression of a number of genes (related to NA or glutathione) involved in root radial transport and in root-to-shoot Zn and Cd translocation in hyperaccumulators (Waters *et al.*, 2006; Deinlein *et al.*, 2012; Haydon *et al.*, 2012). Nicotianamine and glutathione conjugate complexes (GS-X) (Clemens, 2006, 2019) are able to chelate metals and contribute to their root-to-shoot transport in *A. halleri* and *N. caerulescens* (Schat *et al.*, 2002; Deinlein *et al.*, 2012; Tsednee *et al.*, 2014; Cornu *et al.*, 2015). Higher expression of *ZIF1*, encoding a transporter of NA into the vacuole (Haydon *et al.*, 2012), likely contributes to reduced radial transport as well.

Moreover, genes involved in metal remobilization (such as *HMA2* and *NRAMP3*) could play a role in Cd/Zn hypertolerance mechanisms in I16 M (Fig. 3b). *HMA2* drives the outward transport of metals from the cell cytoplasm, possibly enabling Cd/Zn exclusion from sensitive cell-types (Eren & Argüello, 2004; Hanikenne *et al.*, 2008; Lee *et al.*, 2019). *NRAMP3* is involved Mn and Fe remobilization from vacuoles, contributing to the protection of photosynthesis from Cd toxicity (Lanquar *et al.*, 2005; Molins *et al.*, 2013) and was recently associated with a quantitative trait locus (QTL) for intraspecific variation of Zn tolerance in *A. halleri* (Karam *et al.*, 2019).

Despite the use of different Fe concentrations and chelating agents between design 1-Cd and design 2-Zn, many key genes involved in Fe homeostasis were present in the core set of constitutive DEGs between I16 M and I30 NM, confirming the importance of the regulation of Fe in the adaptation to metalliferous soils. In addition to the aforementioned *IRT1* and *NRAMP3* genes, other Fe-transporters showed higher expression in I30 NM (*IRT2*, *NRAMP4*) or I16 M (*VACUOLAR IRON TRANSPORTER-like 1, 5*, Gollhofer *et al.*, 2014; *FERRITIN 2* and *4*, Reyt *et al.*, 2015; and *FRD3*, Roschztardt *et al.*, 2011). In addition, the *PLEIOTROPIC DRUG RESISTANCE 9* (Robe *et al.*, 2021) and *MYB72* (Stringlis *et al.*, 2018) genes, which are involved in the secretion and regulation of Fe-mobilizing coumarins, were more highly expressed in I30 NM than I16 M roots. Finally, *FERRIC REDUCTION OXIDASE 2* (*FRO2*; Satbhai *et al.*, 2017), which is involved in Fe(III) reduction, and *bHLH38* and *bHLH101* transcription factors that are involved in the regulation of Fe-related genes (Gao *et al.*, 2019) also showed higher expression in I30 NM than in I16 M.

Finally, it is remarkable that, so far, none of the major genes associated with hypertolerance and hyperaccumulation in *A. halleri* (e.g. *HMA4*, *MTP1*, *NAS2*) have been found to be differentially expressed between I16 M and I30 NM, suggesting that their high expression is related to the common tolerance trait shared by M and NM populations in this GU.

Modified cell wall structure is associated with different metal accumulation strategies

Transcriptomic data and the analysis of hemicellulose and pectin profiles revealed major differences in cell wall composition

between the two populations (Fig. 4) and may play an important role in the limited metal accumulation strategy of I16 M (Fig. 1d,e). It has been shown that several cell wall genes are induced by metallic stresses in nontolerant species or highly and constitutively expressed in metal hypertolerant genotypes (Herbette *et al.*, 2006; Hassinen *et al.*, 2007; Van De Mortel *et al.*, 2008; Konlechner *et al.*, 2013; Jia-Shi Peng *et al.*, 2016; Leskova *et al.*, 2019).

While total pectin and hemicellulose quantification did not highlight major differences between I16 M and I30 NM (Fig. S3), many specific pectin and hemicellulose epitopes showed higher accumulation in I16 M than in I30 NM roots (Fig. 4c,d). These results confirmed the differences suggested by transcriptomic data and, more importantly, suggested that specific cell wall components are essential for the contrasting Cd accumulation behaviours observed between the two populations (Fig. 4a). Pectins and hemicelluloses are major components of the cell wall that could play an important role in the adaptation to Cd and Zn contamination in soil (Krzyszowska, 2011). Indeed pectins, which are polysaccharides with a negative charge, are able to bind and sequester divalent and trivalent metal ions, such as Cd²⁺ and Zn²⁺ (Krzyszowska, 2011; Loix *et al.*, 2017). The carboxylic groups of pectins are able to bind cations, thus forming a complex with several metals (Pellerin & O'neill, 1998). Given that epidermis, cortex and endodermis root layers are important checkpoints for Cd uptake (Martinka *et al.*, 2014; Barberon, 2017), the abundance and distribution of specific cell wall components in *A. halleri* root may play a major role in Cd entry into the root. Hence, determining cell wall component localisation will be essential to understanding their role in metal accumulation.

Galacturonan, rhamnogalacturonan in particular, gene expression and composition were particularly different between I16 M and I30 NM. Pectin rhamnogalacturonan shows a high affinity for divalent and trivalent metal cations (Yapo, 2011) and might play a major role in the Cd and Zn translocation to the root cortex layer(s) and reduced translocation from the root to the shoot. In strong support of this idea, Cd mainly accumulated in the I16 M root cortex, and in all root tissues of I30 NM (Fig. S4).

It is also interesting to note that several pectinmethylesterase (PME) genes showed higher expression in I16 M than in I30 NM, suggesting that the low level of low-methylesterified pectins in the cell wall could participate in limiting Cd accumulation, as shown for Cu in *Silene* (Rabęda *et al.*, 2015) or for Cd in *Sedum alfredii* (Li *et al.*, 2015).

Lignin related gene-expression and histological staining highlighted some differences between I16 M and I30 NM roots. The induction of monolignols and lignin pathways was reported in plants subjected to toxic metal stress and was related to a defence mechanism that plants activate to strengthen the cell wall and increase rigidity (Herbette *et al.*, 2006). In addition, differences in cell wall composition may contribute to the reduced metal translocation to the shoot, as has been suggested for the La Calamine accession of *N. caerulea* (Van De Mortel *et al.*, 2006; Hanikenne & Nouet, 2011). A major role for lignin in Cd-hyperaccumulation and tolerance in *Sedum plumbizincicola*

has also been suggested (Jia-Shi Peng *et al.*, 2016). The essential role of the cell wall in metal hyperaccumulators was further highlighted by Tao *et al.*, (2017), who proposed a major role of the apoplastic pathways for Cd accumulation in the metal hyperaccumulator *S. alfredii*.

A model for limited metal accumulation strategy in *A. halleri*

Our results support the idea that reduced metal accumulation in the metalicolous I16 M population of *A. halleri* (Fig. 5) is driven by limited metal entry into the root and reduced translocation to the shoot.

I16 M seems to limit Cd and Zn entry into the root via the lower expression of *IRT1*. Moreover, the higher accumulation of specific pectins and hemicelluloses, as well as other modifications of the cell wall structure, can either reinforce the cell wall as a passive barrier or increase its metal-binding capacity and the immobilization of metals in the root, which results in lower translocation to the shoot. Metal confinement to the root is reinforced by the higher expression of genes involved in Cd and Zn vacuolar sequestration in roots and lower expression of genes

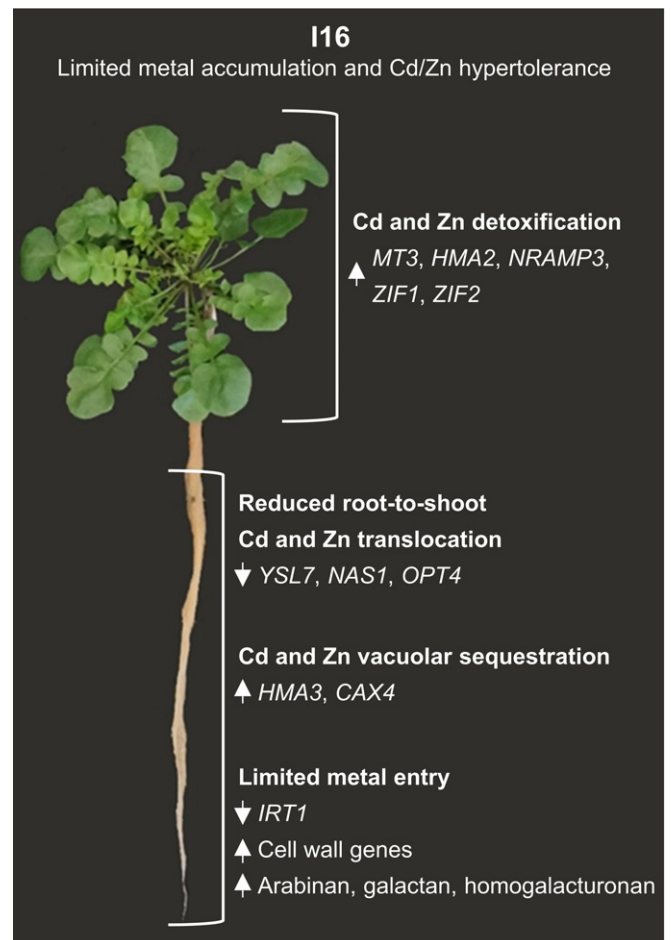


Fig. 5 Model summarizing mechanisms of cadmium exclusion and resistance strategies in the I16 M *Arabidopsis halleri* metalicolous population.

involved in Cd radial transport in roots and root-to-shoot translocation (Fig. 5). The cell wall alterations and regulation of the expression of root transporter genes may account for the overall reduced nutrient uptake in I16 M upon Cd exposure. Our results provide a pioneering model for limited metal accumulation strategies in *A. halleri*.

Acknowledgements

The authors would like to thank Claire-Lyse Meyer for initial discussions and help with the hydroponic culture, Pietro Salis for help during the hydroponic experiment, and Noémie Thiébaud and Marine Joris for technical support during microscopy analyses with Leadmium Green.

This work has benefited from the support of IJPB's Plant Observatory technological platforms. In particular, we thank the imaging and cytology platform for the technical support during confocal microscopy analyses for lignin and cell wall staining. The authors are also grateful to Roman Ceroni, Mauro Abbadini and Erika Cabrini (Fattoria Ariete, Gorno, Italy) for their help with the collection of I16 seeds in Val del Riso (Italy). This work was supported by the FNRS (grants PDR T.0206.13, T0120.18 to MH and NV) and the University of Liège (grant SFRD-12/03 to MH). MH is a Senior Research Associate of the FNRS (Belgium). MC was postdoctoral researcher of the FNRS (1 October 2017 to 30 September 2018). MC is a Research Associate of the INRAE (France). The IJPB benefits from the support of Saclay Plant Sciences-SPS (ANR-17-EUR-0007). VGD is an Advanced Postdoc Fellow from the Swiss National Science Foundation. The authors would like to thank COST Action 19116 'Trace metal metabolism in plants – PLANTMETALS' for supporting the networking between the authors. The authors declare that they have no conflict of interest.

Author contributions

MC, MH and NV designed the research. MC, XA, CYJ, VGD, SS and EM performed the experiments. MC analysed physiological and omic data, and generated all figures and supporting information. MC, CYJ and WW analysed the glycan array data. VGD, XA and MC performed the histological staining and analysed the data. MC wrote the paper, which was extensively edited by NV and MH. All the authors commented on and approved the manuscript.

ORCID

Xinhui An  <https://orcid.org/0000-0003-4089-7003>
 Massimiliano Corso  <https://orcid.org/0000-0002-3243-1660>
 Verónica Gonzalez-Doblas  <https://orcid.org/0000-0002-5476-3228>
 Marc Hanikenne  <https://orcid.org/0000-0002-8964-9601>
 Catherine Yvonne Jones  <https://orcid.org/0000-0001-7121-2236>
 Eugeniusz Malkowski  <https://orcid.org/0000-0001-9804-8114>

M. Sol Schwartzman  <https://orcid.org/0000-0003-4330-1543>
 Nathalie Verbruggen  <https://orcid.org/0000-0003-2296-5404>
 William G. T. Willats  <https://orcid.org/0000-0003-2064-4025>

References

- Arnold PA, Kruuk LEB, Nicotra AB. 2019. How to analyse plant phenotypic plasticity in response to a changing climate. *New Phytologist* **222**: 1235–1241.
- Atmoudjo MA, Hao Z, Mohnen D. 2013. Evolving views of pectin biosynthesis. *Annual Review of Plant Biology* **64**: 747–779.
- Babst-Kostecka A, Schat H, Saumitou-Laprade P, Grodzńska K, Bourceaux A, Pauwels M, Frérot H. 2018. Evolutionary dynamics of quantitative variation in an adaptive trait at the regional scale: the case of zinc hyperaccumulation in *Arabidopsis halleri*. *Molecular Ecology* **27**: 3257–3273.
- Barberon M. 2017. The endodermis as a checkpoint for nutrients. *New Phytologist* **213**: 1604–1610.
- Barberon M, Vermeer JEM, De Bellis D, Wang P, Naseer S, Andersen TG, Humbel BM, Nawrath C, Takano J, Salt DE *et al.* 2016. Adaptation of root function by nutrient-induced plasticity of endodermal differentiation. *Cell* **164**: 447–459.
- Becher M, Talke IN, Krall L, Krämer U. 2004. Cross-species microarray transcript profiling reveals high constitutive expression of metal homeostasis genes in shoots of the zinc hyperaccumulator *Arabidopsis halleri*. *The Plant Journal* **37**: 251–268.
- Bindea G, Mlecnik B, Hackl H, Charoentong P, Tosolini M, Kirilovsky A, Fridman WH, Pagès F, Trajanoski Z, Galon J. 2009. ClueGO: a Cytoscape plug-in to decipher functionally grouped gene ontology and pathway annotation networks. *Bioinformatics* **25**: 1091–1093.
- Blumenkrantz N, Asboe-Hansen G. 1973. New method for quantitative determination of uronic acids. *Analytical Biochemistry* **54**: 484–489.
- Broadley MR, White PJ, Hammond JP, Zelko I, Lux A. 2007. Zinc in plants. *New Phytologist* **173**: 677–702.
- Clemens S. 2006. Toxic metal accumulation, responses to exposure and mechanisms of tolerance in plants. *Biochimie* **88**: 1707–1719.
- Clemens S. 2019. Metal ligands in micronutrient acquisition and homeostasis. *Plant, Cell & Environment* **42**: 2902–2912.
- Clemens S, Aarts MGM, Thomine S, Verbruggen N. 2013. Plant science: the key to preventing slow cadmium poisoning. *Trends in Plant Science* **18**: 92–99.
- Clemens S, Ma JF. 2016. Toxic heavy metal and metalloids accumulation in crop plants and foods. *Annual Review of Plant Biology* **67**: 489–512.
- Cornu J-Y, Deinlein U, Hoereth S, Braun M, Schmidt H, Weber M, Persson DP, Husted S, Schjoerring JK, Clemens S. 2015. Contrasting effects of nicotianamine synthase knockdown on zinc and nickel tolerance and accumulation in the zinc/cadmium hyperaccumulator *Arabidopsis halleri*. *New Phytologist* **206**: 738–750.
- Corso M, Schwartzman MS, Guzzo F, Souard F, Malkowski E, Hanikenne M, Verbruggen N. 2018. Contrasting cadmium resistance strategies in two metalcolous populations of *Arabidopsis halleri*. *New Phytologist* **218**: 283–297.
- Deinlein WU, Weber M, Schmidt H, Rensch S, Trampczynska A, Hansen TH, Husted S, Schjoerring JK, Talke IN, Krämer U *et al.* 2012. Elevated nicotianamine levels in *Arabidopsis halleri* roots play a key role in zinc hyperaccumulation. *The Plant Cell* **24**: 708–723.
- Doblas VG, Geldner N, Barberon M. 2017. The endodermis, a tightly controlled barrier for nutrients. *Current Opinion in Plant Biology* **39**: 136–143.
- Dubeaux G, Neveu J, Zelazny E, Vert G. 2018. Metal sensing by the IRT1 transporter-receptor orchestrates its own degradation and plant metal nutrition. *Molecular Cell* **69**: 953–964.e5.
- Dubois M, Gilles K, Hamilton JK, Rebers PA, Smith F. 1951. A colorimetric method for the determination of sugars. *Nature* **168**: 167.
- Eren E, Argüello JM. 2004. *Arabidopsis* HMA2, a divalent heavy metal transporting P_{1B}-type ATPase, is involved in cytoplasmic Zn²⁺ homeostasis. *Plant Physiology* **136**: 3712–3723.

- Fang X, Gui Z, Lei J, Jiang T, Liu Y, Li GX, Zheng SJ. 2012. Cell wall polysaccharides are involved in P-deficiency-induced Cd exclusion in *Arabidopsis thaliana*. *Planta* 236: 989–997.
- Fasani E, DalCorso G, Varotto C, Li M, Visioli G, Mattarozzi M, Furini A. 2017. The *MTP1* promoters from *Arabidopsis halleri* reveal *cis*-regulating elements for the evolution of metal tolerance. *New Phytologist* 214: 1614–1630.
- Frérot H, Hautekèete N-C, Decombeix I, Bouchet M-H, Créach A, Saumitou-Laprade P, Piquot Y, Pauwels M. 2017. Habitat heterogeneity in the pseudometallophyte *Arabidopsis halleri* and its structuring effect on natural variation of zinc and cadmium hyperaccumulation. *Plant and Soil* 423: 157–174.
- Gao F, Robe K, Gaymard F, Izquierdo E, Dubos C. 2019. The transcriptional control of iron homeostasis in plants: a tale of bHLH transcription factors? *Frontiers in Plant Science* 10: 6.
- Gollhofer J, Timofeev R, Lan P, Schmidt W, Buckhout TJ, Kosman D, Eide D, Broderius M, Fett J, Guerinot M *et al.* 2014. Vacuolar-iron-Transporter1-like proteins mediate iron homeostasis in *Arabidopsis*. *PLoS ONE* 9: e110468.
- Gruber BD, Giehl RFH, Friedel S, Von Wirén N. 2013. Plasticity of the *Arabidopsis* root system under nutrient deficiencies. *Plant Physiology* 163: 161–179.
- Halimaa P, Blande D, Baltzi E, Aarts MGM, Granlund L, Keinänen M, Kärenlampi SO, Kozhevnikova AD, Peräniemi S, Schat H *et al.* 2019. Transcriptional effects of cadmium on iron homeostasis differ in calamine accessions of *Noccaea caerulescens*. *The Plant Journal* 97: 306–320.
- Hanikenne M, Nouet C. 2011. Metal hyperaccumulation and hypertolerance: a model for plant evolutionary genomics. *Current Opinion in Plant Biology* 14: 252–259.
- Hanikenne M, Talke IN, Haydon MJ, Lanz C, Nolte A, Motte P, Kroymann J, Weigel D, Krämer U. 2008. Evolution of metal hyperaccumulation required *cis*-regulatory changes and triplication of *HMA4*. *Nature* 453: 391–395.
- Hassinen V, Tervahauta A, Halimaa P, Plessl M, Peräniemi S, Schat H, Aarts M, Servomaa K, Kärenlampi S. 2007. Isolation of Zn-responsive genes from two accessions of the hyperaccumulator plant *Thlaspi caerulescens*. *Planta* 225: 977–989.
- Haydon MJ, Kawachi M, Wirtz M, Hillmer S, Hell R, Krämer U. 2012. Vacuolar nicotianamine has critical and distinct roles under iron deficiency and for zinc sequestration in *Arabidopsis*. *The Plant Cell* 24: 724–737.
- Herbette S, Tacconat L, Hugouvieux V, Piette L, Magniette M-LM, Cuine S, Auroy P, Richaud P, Forestier C, Bourguignon J *et al.* 2006. Genome-wide transcriptome profiling of the early cadmium response of *Arabidopsis* roots and shoots. *Biochimie* 88: 1751–1765.
- Hosmani PS, Kamiya T, Danku J, Naseer S, Geldner N, Guerinot ML, Salt DE. 2013. Dirigent domain-containing protein is part of the machinery required for formation of the lignin-based Casparian strip in the root. *Proceedings of the National Academy of Sciences, USA* 110: 14498–14503.
- Jan A, Azam M, Siddiqui K, Ali A, Choi I, Haq Q. 2015. Heavy metals and human health: mechanistic insight into toxicity and counter defense system of antioxidants. *International Journal of Molecular Sciences* 16: 29592–29630.
- Karam MJ, Souleman D, Schwartzman MS, Gallina S, Spielmann J, Poncet C, Bouchez O, Pauwels M, Hanikenne M, Frérot H. 2019. Genetic architecture of a plant adaptive trait: QTL mapping of intraspecific variation for tolerance to metal pollution in *Arabidopsis halleri*. *Heredity* 122: 877–892.
- Konlechner C, Türktas M, Langer I, Vaculik M, Wenzel WW, Puschenreiter M, Hauser MT. 2013. Expression of zinc and cadmium responsive genes in leaves of willow (*Salix caprea* L.) genotypes with different accumulation characteristics. *Environmental Pollution* 178: 121–127.
- Krämer U. 2010. Metal hyperaccumulation in plants. *Annual Review of Plant Biology* 61: 517–534.
- Krzyszowska M. 2011. The cell wall in plant cell response to trace metals: polysaccharide remodeling and its role in defense strategy. *Acta Physiologiae Plantarum* 33: 35–51.
- Lanquar V, Lelièvre F, Bolte S, Hamès C, Alcon C, Neumann D, Vansuyt G, Curie C, Schröder A, Krämer U *et al.* 2005. Mobilization of vacuolar iron by AtNRAMP3 and AtNRAMP4 is essential for seed germination on low iron. *EMBO Journal* 24: 4041–4051.
- Lee G, Quintana J, Ahmadi H, Syllwasschly L, Anderson JE, Pietzenuk B, Krämer U. 2019. Enhanced genome integrity maintenance and few large stress-mitigating changes in *Arabidopsis halleri* extreme-habitat local adaptation. *bioRxiv*. doi: 10.1101/859249.
- Leskova A, Zvarík M, Araya T, Giehl RFH. 2019. Nickel toxicity targets cell wall-related processes and PIN2-mediated auxin transport to inhibit root elongation and gravitropic responses in *Arabidopsis*. *Plant and Cell Physiology* 61: 519–535.
- Li T, Tao Q, Shohag MJ, Yang X, Sparks DL, Liang Y. 2015. Root cell wall polysaccharides are involved in cadmium hyperaccumulation in *Sedum alfredii*. *Plant and Soil* 389: 387–399.
- Liu H, Zhao H, Wu L, Liu A, Zhao F-J, Xu W. 2017. Heavy metal ATPase 3 (*HMA3*) confers cadmium hypertolerance on the cadmium/zinc hyperaccumulator *Sedum plumbizincicola*. *New Phytologist* 215: 687–698.
- Loix C, Huybrechts M, Vangronsveld J, Gielen M, Keunen E, Cuypers A. 2017. Reciprocal interactions between cadmium-induced cell wall responses and oxidative stress in plants. *Frontiers in Plant Science* 8: 1867.
- Love MI, Huber W, Anders S. 2014. Moderated estimation of fold change and dispersion for RNA-seq data with DESeq2. *Genome Biology* 15: 550.
- Martinka M, Vaculik M, Lux A. 2014. Plant cell responses to cadmium and zinc. In: Nick P, Opatry Z eds. *Applied plant cell biology, plant cell monographs* 22. Berlin/Heidelberg, Germany: Springer-Verlag, 209–246.
- McCarthy DJ, Chen Y, Smyth GK. 2012. Differential expression analysis of multifactor RNA-Seq experiments with respect to biological variation. *Nucleic Acids Research* 40: 4288–4297.
- Mei H, Cheng NH, Zhao J, Park S, Escareno RA, Pittman JK, Hirschi KD. 2009. Root development under metal stress in *Arabidopsis thaliana* requires the H⁺/cation antiporter CAX4. *New Phytologist* 183: 95–105.
- Merlot S, de la Torre V, Hanikenne M. 2018. Physiology and molecular biology of trace element hyperaccumulation. In: der Ent A, Echevarria G, Baker AJM, Morel JL, eds. *Agromining: farming for metals: extracting unconventional resources using plants*. Cham: Springer International Publishing, 93–116.
- Meyer CL, Juraniec M, Huguet S, Chaves-Rodríguez E, Salis P, Isare M-P, Goormaghtigh E, Verbruggen N. 2015. Intraspecific variability of cadmium tolerance and accumulation, and cadmium-induced cell wall modifications in the metal hyperaccumulator *Arabidopsis halleri*. *Journal of Experimental Botany* 66: 3215–3227.
- Meyer C-L, Pauwels M, Briset L, Godé C, Salis P, Bourceaux A, Souleman D, Frérot H, Verbruggen N. 2016. Potential preadaptation to anthropogenic pollution: evidence from a common quantitative trait locus for zinc and cadmium tolerance in metallophilous and nonmetallophilous accessions of *Arabidopsis halleri*. *New Phytologist* 212: 934–943.
- Molins H, Mchelet L, Lanquar V, Agorio A, Giraudat J, Roach T, Krieger-Liszczay A, Thomine S. 2013. Mutants impaired in vacuolar metal mobilization identify chloroplasts as a target for cadmium hypersensitivity in *Arabidopsis thaliana*. *Plant, Cell & Environment* 36: 804–817.
- Moller I, Marcus SE, Haeger A, Verherbruggen Y, Verhoeff R, Schols H, Ulvskov P, Dalgaard Mikkelsen J, Paul Knox J, Willats W. 2008. High-throughput screening of monoclonal antibodies against plant cell wall glycans by hierarchical clustering of their carbohydrate microarray binding profiles. *Glycoconjugate Journal* 25: 37–48.
- Moller I, Sørensen I, Bernal AJ, Blaukopf C, Lee K, Øbro J, Pettolino F, Roberts A, Mikkelsen JD, Knox JP *et al.* 2007. High-throughput mapping of cell-wall polymers within and between plants using novel microarrays. *The Plant Journal* 50: 1118–1128.
- Parrotta L, Guerriero G, Sergeant K, Cai G, Hausman J-F. 2015. Target or barrier? The cell wall of early- and later-diverging plants vs cadmium toxicity: differences in the response mechanisms. *Frontiers in Plant Science* 6: 133.
- Pauwels M, Vekemans X, Godé C, Frérot H, Castric V, Saumitou-Laprade P. 2012. Nuclear and chloroplast DNA phylogeography reveals vicariance among European populations of the model species for the study of metal tolerance, *Arabidopsis halleri* (Brassicaceae). *New Phytologist* 193: 916–928.
- Pellerin P, O'Neill MA. 1998. The interaction of the pectic polysaccharide Rhamnogalacturonan II with heavy metals and lanthanides in wines and fruit juices. *Analysis Magazine* 26: 32–36.
- Peng J-S, Wang Y-J, Ma GDH-L, Zhang Y-J, Gong J-M. 2016. A pivotal role of cell wall in cadmium accumulation in the Crassulaceae hyperaccumulator *Sedum plumbizincicola*. *Molecular Plant* 10: 771–774.

- Rabęda I, Bilski H, Mellerowicz EJ, Napieralska A, Suski S, Woźny A, Krzesłowska M. 2015. Colocalization of low-methylesterified pectins and Pb deposits in the apoplast of aspen roots exposed to lead. *Environmental Pollution* 205: 315–326.
- Reyt G, Boudouf S, Boucherez J, Gaymard F, Briat JF. 2015. Iron- and ferritin-dependent reactive oxygen species distribution: Impact on *Arabidopsis* root system architecture. *Molecular Plant* 8: 439–453.
- Robe K, Gao F, Lefebvre-legendre L, Sylvestre E, Hem S, Rouhier N, Barberon M, Hecker A, Izquierdo E, Dubos C. 2021. Coumarin accumulation and trafficking in *Arabidopsis thaliana*: a complex and dynamic process. *New Phytologist* 229: 2062–2079.
- Roschzttardtz H, Séguéla-Arnaud M, Briat J-F, Vert G, Curie C. 2011. The FRD3 citrate effluxer promotes iron nutrition between symplastically disconnected tissues throughout *Arabidopsis* development. *The Plant Cell* 23: 2725–2737.
- Satbhai SB, Setzer C, Freynschlag F, Slovak R, Kerdaffrec E, Busch W. 2017. Natural allelic variation of FRO2 modulates *Arabidopsis* root growth under iron deficiency. *Nature Communications* 8: 15603.
- Schat H, Llugany M, Vooijs R, Hartley-Whitaker J, Bleeker PM. 2002. The role of phytochelatin in constitutive and adaptive heavy metal tolerances in hyperaccumulator and non-hyperaccumulator metallophytes. *Journal of Experimental Botany* 53: 2381–2392.
- Schwartzman MS, Corso M, Fataftah N, Scheepers M, Nouet C, Bosman B, Carnol M, Motte P, Verbruggen N, Hanikenne M. 2018. Adaptation to high zinc depends on distinct mechanisms in metallicolous populations of *Arabidopsis halleri*. *New Phytologist* 218: 269–282.
- Shi YZ, Zhu XF, Wan JX, Li GX, Zheng SJ. 2015. Glucose alleviates cadmium toxicity by increasing cadmium fixation in root cell wall and sequestration into vacuole in *Arabidopsis*. *Journal of Integrative Plant Biology* 57: 830–837.
- Stein RJ, Stephan H, Rom J, De MF, Syllwasschy L, Lee G, Garbin L, Clemens S, Kr U. 2016. Relationships between soil and leaf mineral composition are element-specific, environment-dependent and geographically structured in the emerging model *Arabidopsis halleri*. *New Phytologist* 213: 1274–1286.
- Stringlis IA, Yu K, Feussner K, de Jonge R, Van Bentum S, Van Verk MC, Berendsen RL, Bakker PAHM, Feussner I, Pieterse CMJ. 2018. MYB72-dependent coumarin exudation shapes root microbiome assembly to promote plant health. *Proceedings of the National Academy of Sciences, USA* 115: E5213–E5222.
- Su C, Jiang L, Zhang W. 2014. A review on heavy metal contamination in the soil worldwide: situation, impact and remediation techniques. *Environmental Skeptics and Critics* 3: 24–38.
- Tao Q, Jupa R, Luo J, Lux A, Kováč J, Wen Y, Zhou Y, Jan J, Liang Y, Li T. 2017. The apoplasmic pathway via the root apex and lateral roots contributes to Cd hyperaccumulation in the hyperaccumulator *Sedum alfredii*. *Journal of Experimental Botany* 68: 739–751.
- Tóth G, Hermann T, Da Silva MR, Montanarella L. 2016. Heavy metals in agricultural soils of the European Union with implications for food safety. *Environment International* 88: 299–309.
- Tsednee M, Yang S-C, Lee D-C, Yeh K-C. 2014. Root-secreted nicotianamine from *Arabidopsis halleri* facilitates zinc hypertolerance by regulating zinc bioavailability. *Plant Physiology* 166: 839–852.
- Ursache R, Andersen TG, Marhavý P, Geldner N. 2018. A protocol for combining fluorescent proteins with histological stains for diverse cell wall components. *The Plant Journal* 93: 399–412.
- Van De Mortel JE, Schat H, Moerland PD, Van Themaat EVL, Van Der Ent S, Blankestijn H, Ghandilyan A, Tsiatsiani S, Aarts MGM. 2008. Expression differences for genes involved in lignin, glutathione and sulphate metabolism in response to cadmium in *Arabidopsis thaliana* and the related Zn/Cd-hyperaccumulator *Thlaspi caerulescens*. *Plant, Cell & Environment* 31: 301–324.
- Van De Mortel JE, Villanueva LA, Schat H, Kwekkeboom J, Coughlan S, Moerland PD, Ver E, Van Themaat L, Koornneef M, Aarts MGM. 2006. Large expression differences in genes for iron and zinc homeostasis, stress response, and lignin biosynthesis distinguish roots of *Arabidopsis thaliana* and the related metal hyperaccumulator *Thlaspi caerulescens*. *Plant Physiology* 142: 1127–1147.
- Verbruggen N, Hermans C, Schat H. 2009. Molecular mechanisms of metal hyperaccumulation in plants. *New Phytologist* 181: 759–776.
- Verbruggen N, Juraniec M, Baliardini C, Meyer C-L. 2013. Tolerance to cadmium in plants: the special case of hyperaccumulators. *BioMetals* 26: 633–638.
- Verhertbruggen Y, Marcus SE, Chen J, Knox JP. 2013. Cell wall pectic arabinans influence the mechanical properties of *Arabidopsis thaliana* inflorescence stems and their response to mechanical stress. *Plant Cell Physiology* 54: 1278–1288.
- Vert G, Grotz N, Dédaldéchamp F, Gaymard F, Lou GM, Briat J-F, Curie C. 2002. IRT1, an *Arabidopsis* transporter essential for iron uptake from the soil and for plant growth. *The Plant Cell* 14: 1223–1233.
- Wasowicz P, Pauwels M, Pasierbinski A, Przedpelska-Wasowicz EM, Babst-Kostecka AA, Saumitou-Laprade P, Rostanski A. 2016. Phylogeography of *Arabidopsis halleri* (Brassicaceae) in mountain regions of Central Europe inferred from cpDNA variation and ecological niche modelling. *PeerJ* 4: e1645.
- Waters BM, Chu H-H, Didonato RJ, Roberts LA, Easley RB, Lahner B, Salt DE, Walker EL. 2006. Mutations in *Arabidopsis Yellow Stripe-Like1* and *Yellow Stripe-Like3* reveal their roles in metal ion homeostasis and loading of metal ions in seeds. *Plant Physiology* 141: 1446–1458.
- Yapo BM. 2011. Pectin Rhamnogalacturonan II: on the 'small stem with four branches' in the primary cell walls of plants. *International Journal of Carbohydrate Chemistry* 2011: 1–11.
- Zhong H, Lauchli A. 1993. Changes of cell wall composition and polymer size in primary roots of cotton seedlings under high salinity. *Journal of Experimental Botany* 44: 773–778.

Supporting Information

Additional Supporting Information may be found online in the Supporting Information section at the end of the article.

Fig. S1 Geographical origin and mineral element quantification of *Arabidopsis halleri* plants grown at their native site.

Fig. S2 Validation of RNA-Seq results by real-time quantitative polymerase chain reaction (qRT-PCR) analysis.

Fig. S3 Pectin and hemicellulose content in *Arabidopsis halleri* roots.

Fig. S4 Cadmium distribution in *Arabidopsis halleri* roots.

Table S1 Composition of the hydroponic solutions used in this study.

Table S2 Sequences of qRT-PCR primers used in this study.

Table S3 RNA-Seq transcriptomic data of I16 M and I30 NM populations.

Please note: Wiley Blackwell are not responsible for the content or functionality of any Supporting Information supplied by the authors. Any queries (other than missing material) should be directed to the *New Phytologist* Central Office.